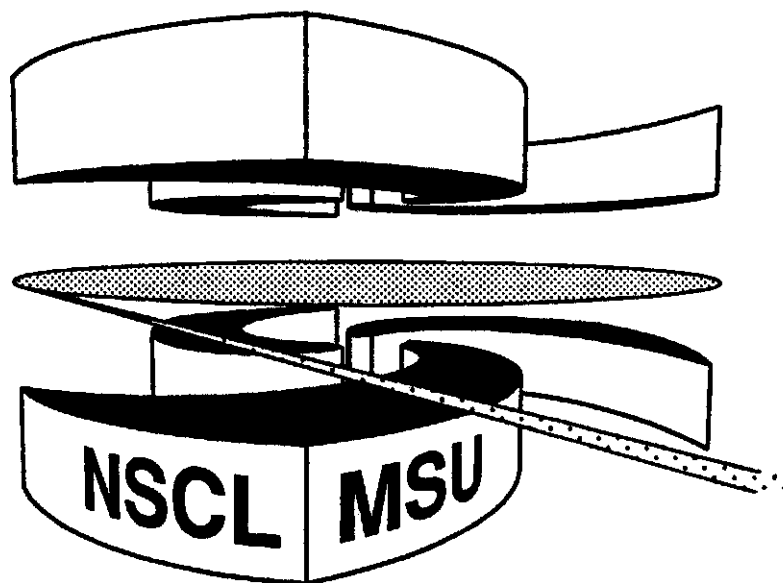


**MICHIGAN STATE
UNIVERSITY**

National Superconducting Cyclotron Laboratory

**FIRST OBSERVATION OF AN EXCITED STATE IN THE
NEUTRON-RICH NUCLEUS ^{31}Na**

**B.V. PRITYCHENKO, T. GLASMACHER, B.A. BROWN,
P.D. COTTLE, R.W. IBBOTSON, K.W. KEMPER, L.A. RILEY,
H. SCHEIT**



MSUCL-1156

JUNE 2000

First observation of an excited state in the neutron-rich nucleus

^{31}Na

B. V. Pritychenko^{1,2}, T. Glasmacher^{1,2}, B.A. Brown^{1,2}, P.D. Cottle³, R.W. Ibbotson^{1*},
K.W. Kemper³, L.A. Riley⁴, H. Scheit^{1,2†}

¹ *National Superconducting Cyclotron Laboratory, Michigan State University, East Lansing,
Michigan 48824*

² *Department of Physics and Astronomy, Michigan State University, East Lansing, Michigan
48824*

³ *Department of Physics, Florida State University, Tallahassee, Florida 32306*

⁴ *Department of Physics and Astronomy, Earlham College, Richmond, Indiana 47374*

(June 6, 2000)

Abstract

The first excited state in the neutron-rich $N = 20$ isotope ^{31}Na was observed at **350(20) keV** via intermediate energy heavy-ion scattering, which is dominated by the Coulomb excitation mechanism. This state appears to be a rotational excitation built on a strongly deformed ground state. The yield of the γ -ray de-exciting this state can be reproduced by a shell model calculation

*Present address: Brookhaven National Laboratory, Upton, New York 11973

†Present address: Max-Planck-Institut für Kernphysik, Postfach 10 39 80, D-69029 Heidelberg, Germany

which takes $\nu(f_{7/2}, p_{3/2})$ intruder configurations into account.

The observation of strong deformation in neutron-rich isotopes at or near the $N = 20$ shell closure serves as an important illustration that the structure of nuclei changes as isospin increases when compared to nuclei near the valley of β -stability. The first evidence for strong deformation in these nuclei was the observation of nuclear binding energies that were too large to be understood in the context of conventional shell model calculations [1–4]. More recently, intermediate energy Coulomb excitation measurements of the $B(E2; 0_{gs}^+ \rightarrow 2_1^+)$ value in the neutron-rich $N = 20$ nucleus ^{32}Mg yielded a result that implied a large degree of collectivity [5,6]. Shell model calculations including neutron $\nu(fp)$ “intruder” configurations [7–13] as well as calculations in other frameworks [14–18] have been performed to gain an understanding of these observations.

In the present letter, we report the results of an intermediate energy heavy-ion scattering measurement of the $N = 20$ nucleus ^{31}Na , which has eight more neutrons than the stable sodium isotope ^{23}Na . This reaction is dominated by the Coulomb excitation mechanism in ^{31}Na , although our calculations indicate a substantial contribution from the nuclear interaction. We observed the first excited state in this nucleus and measured the cross section for populating this state at small scattering angles using in-beam γ -ray spectroscopy. The results indicate that ^{31}Na is comparable in collectivity to its even-even isotone ^{32}Mg . The data can be reproduced by a shell model calculation based upon $\nu(f_{7/2}, p_{3/2})$ intruder configurations.

Intermediate energy heavy-ion scattering has been used to determine excitation energies and electromagnetic matrix elements in a variety of radioactive nuclei (for a review, see [19]). In this technique, a beam of radioactive nuclei - generally with laboratory-frame kinetic energies of greater than 30 MeV/nucleon - are scattered from a high- Z target (typically gold or lead). The projectile nucleus can be excited by either Coulomb or nuclear forces; however, at small scattering angles ($\theta_{lab} < 4.0^\circ$ at 50 MeV/nucleon) Coulomb excitation dominates the inelastic scattering process. Hence, the electromagnetic properties of the projectile nucleus can be studied by measuring the γ -rays emitted by projectiles which are scattered into small angles.

The present measurement of ^{31}Na was performed at the National Superconducting Cyclotron Laboratory (NSCL) at Michigan State University. The ^{31}Na beam was produced via fragmentation of a primary 80 MeV/nucleon ^{48}Ca beam from the NSCL superconducting electron cyclotron resonance ion source and the K1200 superconducting cyclotron. The primary beam had an intensity of 8 particle nA. Fragmentation of the primary beam took place in a thick (376 mg/cm^2) ^9Be target located at the mid-acceptance target position of the A1200 fragment separator [20]. The energy of the ^{31}Na particles produced in the fragmentation reaction was 58.9 MeV/nucleon.

A gold foil of thickness 702 mg/cm^2 was used as the secondary target. After passing through the gold foil, the secondary beam particles (including ^{31}Na) were stopped in a cylindrical fast-slow phoswich detector (called the “zero-degree detector”, or ZDD) which allowed nuclear charge identification of the secondary beam particles. The ZDD only detected secondary beam particles scattered into laboratory angles of less than 2.80° . Time-of-flight measurements in the beam line and charge identification in the ZDD provided positive isotope identification. The beam rate for ^{31}Na measured in the ZDD was only 3 particles/s, and 1,280,000 ^{31}Na particles were collected in total. The NSCL NaI(Tl) array [21] was used to detect photons in coincidence with the scattered beam particles.

The γ -ray spectrum in coincidence with the detection of ^{31}Na particles in the ZDD is shown in Fig. 1. The left panel shows the spectrum without correcting for the Doppler shift of γ -rays emitted from the moving ^{31}Na projectiles (that is, the spectrum as seen in the laboratory frame), while the panel on the right includes this correction (the spectrum as seen in the rest frame of the projectile). The clearest feature in the Doppler-shifted spectrum is a γ -ray peak at $350 \pm 20\text{ keV}$. Given the small beam rate for ^{31}Na in this experiment ($\approx 3\text{ ions/s}$), the clarity of the 350 keV peak demonstrates the sensitivity of the present experimental arrangement. Based on the known ground state spin of ^{31}Na (which was determined by Huber *et al.* [22] to be $J = 3/2$) and the nature of the reaction used here (arguments 19 and 20 in [23]) we propose that the 350 keV γ -ray de-excites the first excited state (with $J = 5/2$) in a $K = 3/2$ rotational band built on the ground state.

The yield in the 350 keV peak is analyzed to obtain a cross section of 115 ± 32 mb for producing this γ -ray. The error on the cross section (115 ± 32 mb, 25%) is an experimental error, taking into account systematic and statistical uncertainties in the experiment. In this particular experiment the statistical error is dominant. This analysis of the yield - which is described in detail in [19] - assumes that the angular distribution of this de-excitation γ -ray is that of a pure $M1$ transition (while the excitation in intermediate energy Coulomb excitation is purely $E2$ in character). The transition probability for an $M1$ transition with even a modest $B(M1; 5/2^+ \rightarrow 3/2^+)$ value ($\approx 0.05 \mu_N^2$) is much larger than that of a strong $E2$ transition. Admixtures of an $E2$ multipolarity would only introduce a small additional error. The present analysis also includes corrections for γ -ray absorption in the target, which in turn depends on the lifetime of the $J = 5/2$ state (and, therefore, on the range of locations of the ^{31}Na nuclei when they decay). For this, a half-life of 15 ps was assumed, which corresponds to $B(M1; 5/2^+ \rightarrow 3/2^+) = 0.06 \mu_N^2$, a result from a shell model calculation described below. The corrections for absorption in the target do not depend very sensitively on the assumed lifetime. The extreme cases of instantaneous decay and a life time so long that the Doppler shift correction no longer would work give efficiencies which are 11% lower and 5% higher, respectively.

It is quite likely that the $J = 7/2$ member of the rotational band is also populated in the present reaction since the $E2$ matrix element connecting this state to the ground state would be comparable to that connecting the $J = 5/2$ state to the ground state. Therefore, the feeding of the $5/2$ state by the $7/2$ state must be considered when extracting a cross section for direct population of the $5/2$ state from the yield of the 350 keV γ -ray. (Multiple excitations - coupled channels effects - are small in reactions such as this one [19], so we can limit our consideration to states which would be populated in single step excitations).

We estimate the energy of the $J = 7/2$ state using a shell model calculation which was performed for ^{31}Na using the same $sd - pf$ Hamiltonian and model space that was used in [24–26] for the neutron-rich Si, S and Ar isotopes. The calculations discussed in this paper are based upon a pure $2p - 2h$ ($2\hbar\omega$) neutron configuration - the configuration which is

responsible for the strong deformation in ^{32}Mg . The allowed $2\hbar\omega$ neutron configurations were $(d_{5/2})^6(d_{3/2}, s_{1/2})^4(f_{7/2}, p_{3/2})^2$, and the allowed proton configurations were $d_{5/2}^3$ and $d_{5/2}^2(s_{1/2}, d_{3/2})$. This calculation yields an energy of 1525 keV for the $J = 7/2$ state, 197 keV for the $J = 5/2$ state, and positive parity for the band.

Of course, the hypothesized $J = 7/2$ state at 1525 keV can de-excite to the ground state via an $E2$ transition; however, the shell model calculation predicts a strong $B(M1; 7/2^+ \rightarrow 5/2^+)$ value ($0.26 \mu_N^2$). This matrix element, together with the predicted $B(E2; 7/2^+ \rightarrow 3/2^+) = 43 e^2\text{fm}^4$ and $B(E2; 7/2^+ \rightarrow 5/2^+) = 14 e^2\text{fm}^4$, gives the result that 95% of the decays from the $7/2$ state go to the $5/2$ state. It is worth noting that the branch ratio to the $5/2$ state is quite large even if the $B(M1; 7/2^+ \rightarrow 5/2^+)$ matrix element is much smaller. For example, even if $B(M1; 7/2^+ \rightarrow 5/2^+) = 0.05 \mu_N^2$, the $7/2$ state decays with a 77% branch to the $5/2$ state.

The results of our shell model calculations are in agreement with those of Caurier *et al.* [12], who predicted that transition energy for the first excited state in ^{31}Na is ~ 200 keV. With the recent change [27] of the cross-shell interaction, the authors of Ref. [12] predict the $5/2^+$ state at 284 keV and the $7/2^+$ state at 1050 keV.

While there is no evidence in the experimental spectrum for a γ -ray in the vicinity of the energy we expect for the $7/2 \rightarrow 5/2$ transition (≈ 1175 keV or ≈ 700 keV), the experimentally observed background is consistent with the expected yields of 4 (or 5) counts, respectively.

The shell model calculations presented here and the ones of Ref. [12] predict only two excited states below an excitation energy of 2 MeV, the $5/2^+$ state and the $7/2^+$ state. One can envision a scenario where the $5/2^+$ state is located slightly below the experimental energy threshold of 160 keV and the $7/2^+$ state is at around 510 keV. In this scenario, the 350 keV γ -ray would correspond to the $7/2^+ \rightarrow 5/2^+$ transition. But to reproduce the experimentally observed excitation cross section of 115 ± 32 mb to the presumed $7/2^+$ state, a value $\beta_2 \approx 0.94$ would be required, which is extremely unlikely. Thus we conclude that the 350 keV γ -ray corresponds to the $5/2^+$ to ground state transition.

The present shell model calculation predicts values for electromagnetic matrix elements connecting members of the ground state rotational band, but a reaction model is necessary to translate the shell model predictions into experimental cross sections for the 5/2 and 7/2 states in the present scattering experiment. We used the coupled channels code ECIS88 [28] with an optical model parameter set determined for the $^{17}\text{O}+^{208}\text{Pb}$ reaction at 84 MeV/nucleon [29] to calculate the angular distributions with an average beam energy of 51.5 MeV/nucleon. We integrated the angular distribution out to the maximum scattering angle encountered in the experiment ($\theta_{\text{max}}^{\text{lab}} = 2.8^\circ$) and adopted a form factor corresponding to a static axial quadrupole deformation. The results of these calculations are summarized in Table 1. There are two deformation parameters involved in this calculation. The first, the ‘‘Coulomb deformation’’ β_C , reflects the deformation of the proton density in the nucleus and corresponds to the electromagnetic matrix element $B(E2; I_{gs} \rightarrow I_f)$. In the rotational model [30], $B(E2; I_{gs} \rightarrow I_f)$ and β_C are related to first order via the equations

$$B(E2; I_i \rightarrow I_f) = Q_0^2 \frac{5}{16\pi} \langle I_i K 2 0 | I_f K \rangle^2 \quad (1)$$

and

$$Q_0 = \left(\frac{16\pi}{5}\right)^{1/2} \frac{3}{4\pi} Z e R_0^2 \beta, \quad (2)$$

where Q_0 is the intrinsic quadrupole moment. The radius R_0 is given by $R_0 = r_0 A^{1/3}$, where we take $r_0 = 1.20$ fm. For the 5/2⁺ state, the shell model result ($B(E2; 3/2 \rightarrow 5/2) = 196 e^2\text{fm}^4$) gives a prediction of $\beta_C = 0.51$. In the case of the 7/2 state, the shell model calculation gives $B(E2; 3/2 \rightarrow 7/2) = 87.5 e^2\text{fm}^4$, so that $\beta_C = 0.46$.

The second deformation parameter in the calculation is the ‘‘nuclear matter deformation parameter’’ β_A . While the Coulomb deformation parameter is used to calculate the electromagnetic interaction between target and projectile, the nuclear deformation parameter is used to determine the interaction via the nuclear force. In the isoscalar collective model, the neutron and proton densities are assumed to have the same deformation. In such a case, the nuclear matter deformation parameter could be set as $\beta_A = \beta_C$. However, the present

shell model calculations yield results for neutron and proton transition multipole matrix elements which are different from the standard collective model picture. To account for these calculated matrix elements and the *rms* proton and neutron radii calculated in Ref. [31], β_A is set to 0.47 for both the $3/2_{gs} \rightarrow 5/2$ and $3/2_{gs} \rightarrow 7/2$ excitations.

The coupled channels calculations using these deformation parameters yield cross sections of 54 mb for the 5/2 state and 27 mb for the 7/2 state. If 95% of the decays of the 7/2 state go to the 5/2 state, the cross section for producing the 350 keV γ -ray would be 80 mb. Since the experimental result is 115 ± 32 mb, we conclude that the shell model calculations are consistent with the measurement.

One issue relevant to this study is understanding the role of the nuclear interaction in the scattering reaction measured here. The top panel of Fig. 2 shows the nuclear and Coulomb contributions to the angular distribution for the $J = 5/2$ state calculated with the shell model results. The nuclear interaction accounts for $\approx 15\%$ of the cross section for the angular range detected in this experiment. Coulomb excitation plays the dominant role in this experiment, but scattering via the nuclear force cannot be neglected.

Motobayashi et al. [5] fit their data on ^{32}Mg using the standard rotational model (where the proton and neutron deformations are equal) to directly extract a quadrupole deformation parameter β_2 . We can analyze our ^{31}Na with the same prescription by assuming that $\beta_C = \beta_A$, that the deformation parameters for the 5/2 and 7/2 states are equal, and that 95% of the de-excitations of the 7/2 state go to the 5/2 state. The result, $\beta_2 = 0.59 \pm 0.08$, is close to the deformation parameters obtained for ^{32}Mg by both Motobayashi *et al.* [5] and Pritychenko *et al.* [6]. Taking into account the possibility of isovector deformation predicted by the shell model compared to isoscalar deformation only, introduces an additional uncertainty of 0.06 in β_2 . Thus the deformation parameter is $\beta_2 = 0.59 \pm 0.08(\text{experimental}) \pm 0.06(\text{theoretical}) = 0.59 \pm 0.10$. The nuclear and Coulomb contributions to this calculation are given in Table I and shown in the bottom panel of Fig. 2.

In the analyses we have used here, we have discussed the relationship between β_A and β_C (equivalently, the relationship between the proton and neutron deformations). However,

since Coulomb excitation dominates the scattering process described here, the most reliable inferences that can be taken from the present work are those about the role of the protons. To determine the role of the neutrons in the excitation studied here, a different experimental probe, such as proton scattering in inverse kinematics (< 50 MeV/nucleon), must be used. Such a measurement would not only determine the difference between the proton and neutron multipole moments, but would also provide insights about the mechanisms involved in the relationship between proton and neutron densities, such as core polarization [32]. Proton scattering from beams of radioactive nuclei has been demonstrated for several *sd* and *f* shell nuclei recently [33–37]. While a beam intensity of 1000 particles/sec is required for such an experiment, it is likely that such an intensity will be available for ^{31}Na at radioactive beam facilities now under construction. This discussion applies equally well to the even-even isotone ^{32}Mg .

In summary, we have made the first observation of an excited state (at 350 keV) in the neutron-rich nucleus ^{31}Na using intermediate energy heavy-ion scattering, which is dominated by the Coulomb interaction. This state appears to be the first rotational excitation ($J = 5/2$) of a band built on the $J = 3/2$ ground state. The population of the 350 keV state can be reproduced using a shell model calculation which takes $\nu(f_{7/2}, p_{3/2})$ intruder configurations into account, as long as feeding of this state by the $J = 7/2$ state is considered. We have also used the rotational model to determine a best fit deformation parameter, $\beta_2 = 0.59 \pm 0.10$. This deformation parameter is comparable to that in the even-even $N = 20$ isotone ^{32}Mg .

This work was supported by the National Science Foundation through grant numbers PHY-9528844, PHY9605207, PHY-9875122 and PHY-9970991.

REFERENCES

- [1] C. Thibault *et al.*, Phys. Rev. **C12**, 644 (1975).
- [2] W. Chung and B.H. Wildenthal, Phys. Rev. **C22**, 2260 (1980).
- [3] C. Détraz *et al.*, Nucl. Phys. **A394**, 378 (1983).
- [4] D.J. Viera *et al.*, Phys. Rev. Lett. **57**, 3253 (1986).
- [5] T. Motobayashi *et al.*, Phys. Lett. B **346**, 9 (1995).
- [6] B.V. Pritychenko *et al.*, Phys. Lett. B **461**, 322 (1999).
- [7] A. Watt *et al.*, J. Phys. G **7**, L145 (1981).
- [8] A. Poves and J. Retamosa, Phys. Lett. B **184**, 311 (1987).
- [9] E.K. Warburton, J.A. Becker and B.A. Brown, Phys. Rev. **C41**, 1147 (1990).
- [10] N. Fukunishi, T. Otsuka and T. Sebe, Phys. Lett. B **296**, 279 (1992).
- [11] A. Poves and J. Retamosa, Nucl. Phys. **A571**, 221 (1994).
- [12] E. Caurier *et al.*, Phys. Rev. **C58**, 2033 (1998).
- [13] Y. Utsuno, T. Otsuka, T. Mizusaki, and M. Honma, Phys. Rev. **C60**, 054315 (1999).
- [14] X. Campi *et al.*, Nucl. Phys. **A251**, 193 (1975).
- [15] K. Heyde and J.L. Wood, J. Phys. G **17**, 135 (1991).
- [16] Z. Ren *et al.*, Phys. Lett. B **380**, 241 (1996).
- [17] J. Terasaki *et al.*, Nucl. Phys. **A621**, 706 (1997).
- [18] G.A. Lalazissis, A.R. Farhan, and M.M. Sharma, Nucl. Phys. **A628**, 221 (1998).
- [19] T. Glasmacher, Annu. Rev. Nucl. Part. Sci. **48**, 1 (1998).
- [20] B.M. Sherrill *et al.*, Nucl. Instr. Meth. **B56**, 1106 (1991).

- [21] H. Scheit *et al.*, Nucl. Instr. Meth. **A422**, 124 (1999).
- [22] G. Huber *et al.*, Phys. Rev. **C18**, 2342 (1978).
- [23] J.K. Tuli, Nucl. Data Sheets **86**, ix (1999).
- [24] H. Scheit *et al.*, Phys. Rev. Lett. **77**, 3967 (1996).
- [25] T. Glasmacher *et al.*, Phys. Lett. B **395**, 163 (1997).
- [26] R.W. Ibbotson *et al.*, Phys. Rev. Lett. **80**, 2081 (1998).
- [27] A. Poves, priv. comm. 1999.
- [28] J. Raynal, Computer code ECIS88, unpublished.
- [29] R. Ligouri Neto *et al.*, Nucl. Phys. A **560**, 733 (1993).
- [30] P. Ring and P. Schuck, The Nuclear Many-Body Problem, (Springer-Verlag, New York, 1980).
- [31] B.A. Brown and W.A. Richter, Phys. Rev. **C54**, 673 (1996).
- [32] B. A. Brown, A. Arima and J. B. McGrory, Nucl. Phys. **A277**, 77 (1977).
- [33] G. Kraus *et al.*, Phys. Rev. Lett. **73**, 1773 (1994).
- [34] J.H. Kelley *et al.*, Phys. Rev. **C56**, R1206 (1997).
- [35] L.A. Riley *et al.*, Phys. Rev. Lett. **82**, 4196 (1999).
- [36] J.K. Jewell *et al.*, Phys. Lett. B **454**, 181 (1999).
- [37] F. Maréchal *et al.*, Phys. Rev. C **60**, 034615 (1999).

TABLES

TABLE I. Excitation cross sections (integrated over $\theta_{\text{cm}} < 3.25^\circ$) for states in ^{31}Na from coupled channels calculations with the optical model parameter set determined for the $^{17}\text{O}+^{208}\text{Pb}$ reaction at 84 MeV/nucleon [29]. The shell model predicts a total cross section of about 80 mb, which needs to be compared to the measured cross section of 115 ± 32 mb. In the "Fit to data" the deformation parameters β_C and β_A have been adjusted to reproduce the measured cross section.

Transition	σ_{Coul} (mb)	σ_{Nucl} (mb)	$\sigma_{\text{Coul+Nucl}}$ (mb)	β_C	β_A
Shell model					
$3/2 \rightarrow 5/2$	49.1	7.8	54.2	0.510	0.470
$3/2 \rightarrow 7/2$	23.7	5.0	27.3	0.460	0.470
Fit to data					
$3/2 \rightarrow 5/2$	64.9	11.7	73.1	0.59(10)	0.59(10)
$3/2 \rightarrow 7/2$	39.4	7.5	44.6	0.59(10)	0.59(10)

FIGURES

$^{31}\text{Na} + ^{197}\text{Au}$

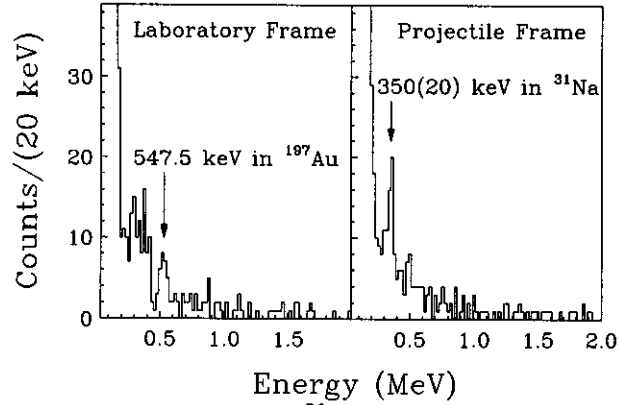


FIG. 1. In-beam photon spectrum gated on ^{31}Na . The left panel shows the spectrum without Doppler correction as measured in the laboratory with the $7/2^+ \rightarrow 3/2^+$ transition in the gold target visible as a peak. The right panel shows the spectrum after event-by-event Doppler correction in the projectile frame. The $350(20) \text{ keV } (5/2^+) \rightarrow 3/2^{(+)}$ transition in ^{31}Na becomes visible as a peak.

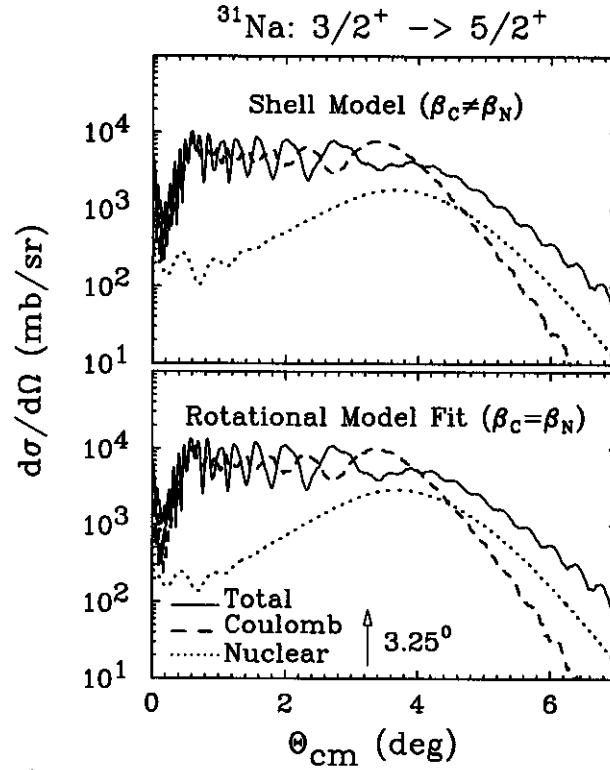


FIG. 2. Angular distributions of the scattered projectile in the first excited state in ^{31}Na at 350 keV calculated using the coupled channels code ECIS88. The top panel shows the results using deformation parameters β_A and β_C from the shell model calculation. The results with the standard rotational model fit (assuming $\beta_A = \beta_C$ and adjusting these to reproduce the measured cross section) are shown in the bottom panel.